Available online at www.sciencedirect.com
ScienceDirect
Journal of Organometallic Chemistry 692 (2007) 4784–4791
Journal of Organometallic Chemistry
www.elsevier.com/locate/jorganchem

Comparing propene polymerization with 1-butene polymerization catalyzed by MAO-activated C_2- and C_1-symmetric zirconocenes: An experimental and computational study on the influence of olefin size on stereoselectivity

Pierluigi Mercandelli [a,*], Angelo Sironi [a], Luigi Resconi [b,*], Isabella Camurati [b]

[a] *Dipartimento di Chimica Strutturale, Università di Milano, via Venezian 21, I-20133 Milano, Italy*
[b] *Basell Polyolefins, Centro Ricerche G. Natta, I-44100 Ferrara, Italy*

Received 4 May 2007; received in revised form 14 June 2007; accepted 14 June 2007
Available online 23 June 2007

Dedicated to Professor Gerhard Erker on the occasion of his 60th birthday.

Abstract

Polypropene and poly(1-butene) have been synthesized under very similar experimental conditions with a series of MAO-activated C_2-symmetric and C_1-symmetric *ansa*-zirconocenes. The C_1-symmetric zirconocenes bearing the bilaterally symmetric fluorenyl or bis(2-methylthieno)cyclopentadienyl ligand connected through a dimethylsilyl bridge to substituted indenyl ligands produce isotactic polybutene of similar or higher molecular mass and with noticeably higher isotacticity, compared to isotactic polypropene prepared with the same catalysts under comparable conditions. Structural and mechanistic reasons for such behavior are discussed on the basis of QM/MM calculations.

Keywords: Isotactic polypropylene; Isotactic polybutene; QM/MM calculations; ^{13}C NMR; Metallocene catalysts; Stereoselective olefin polymerization

1. Introduction

Stereoselectivity in olefin polymerization is ruled by site control, chain end control being by far less effective and apparent only at low temperature when chiral information from the active metal site is missing [1]. While the influence of catalyst symmetry, temperature, monomer concentration, the metal and the type of cocatalyst on enantioselectivity have been extensively investigated, studies on the influence of monomer size on the polymer stereoregularity have been limited. Herfert and Fink have shown that Ewen's C_1-symmetric $Me_2C(3\text{-}MeCp)(9\text{-}Flu)ZrCl_2$, which is close to perfectly hemiisospecific in propene polymerization (*mmmm* ~19%), becomes slightly isoselective in the case of 1-butene, producing PB with 46% *mmmm* [2], likely because the larger olefin substituent, thus the bulkier growing chain, increases the rate of site isomerization to the less hindered coordination site: the monomer has then a higher chance of coordination and insertion at the more isoselective site. In addition to this example, a (small) increase of enantioface selectivity in 1-butene vs. propene has been noted before also in the case of site control with C_2-symmetric metallocenes [3,4], and in the case of chain end control [5,6].

We have recently reported on the polymerization of propene [7] and 1-butene [8] with a series of C_1-symmetric and C_2-symmetric zirconocenes. Possibly, the most striking feature of the C_1-symmetric catalysts is the strong increase in catalyst selectivity on going from propene to

* Corresponding authors. Tel.: +39 02 503 14447; fax: +39 02 503 14454 (P. Mercandelli); tel.: +39 0532 468368 (L. Resconi).
E-mail addresses: pierluigi.mercandelli@unimi.it (P. Mercandelli), luigi.resconi@basell.com (L. Resconi).

0022-328X/$ - see front matter © 2007 Elsevier B.V. All rights reserved.
doi:10.1016/j.jorganchem.2007.06.021

1-butene. Here we report an updated set of propene and 1-butene polymerization results and an attempt at rationalizing the observed differences by means of QM/MM modeling.

2. Results and discussion

2.1. Polymerization results

Selected literature polypropene [7] and polybutene [8] characterization data from known complexes are compared in Table 1. In addition to the data already presented in Refs. [7,8], we have produced and analyzed polypropene and polybutene samples with three additional C_1-symmetric zirconocenes, namely Me_2Si(2-MeInd)(9-Flu)$ZrCl_2$ (**2**) [9], Me_2Si(2,4,6-Me_3Ind)(9-Flu)$ZrCl_2$ (**3**) and Me_2Si[2-Me-4-(α-naphthyl)Ind](BMTCp)$ZrCl_2$ (BMTCp = bis(2-methylthieno)cyclopentadienyl). The latter complex, for which only iPP results were previously presented [7], is the most stereoselective among the C_1-symmetric structures also in 1-butene polymerization, producing iPB with the highest stereoregularity (*mmmm* = 98%), and a consequently high melting point (T_m = 109 °C for the crystalline form II), values almost identical to those obtained with the most isoselective C_2-symmetric complex *rac*-H_2C-(3-^{t}BuInd)$_2ZrCl_2$ [8]. We also prepared and tested Me_2Si(2,4,6-Me_3Ind)(9-Flu)$ZrMe_2$ (**3a**), the dimethyl derivative of **3** [10]. **3a** was originally prepared in order to generate a more soluble (hence easier to purify) version of **3**. As a matter of fact, **3a** is soluble in pentane, a striking difference with respect to **3** which is sparingly soluble even in dichloromethane. The results listed in Table 1 clearly show that **3** and **3a** give identical polymers, and provide additional support to the fact that a dichloro metallocene and its dimethyl analogue give rise to catalytically identical active species upon activation with MAO.

The observed isoselectivity (in terms of the polymer % *mm* triads) of the selected zirconocenes for propene vs. 1-butene is plotted in Fig. 1. As expected [3,4], the C_2-symmetric zirconocenes *rac*-Me_2Si(2-MeInd)$_2ZrCl_2$ (**1**), *rac*-Me_2Si(2-MeBenz[e]Ind)$_2ZrCl_2$ and *rac*-H_2C(3-^{t}BuInd)$_2ZrCl_2$, that are already highly isoselective for propene polymerization, show a small increase in stereoselectivity on going from propene to 1-butene. On the other hand, the C_1-symmetric catalysts show a much more pronounced increase in selectivity on going to the larger monomer, with the fluorenyl-based complexes showing the largest difference.

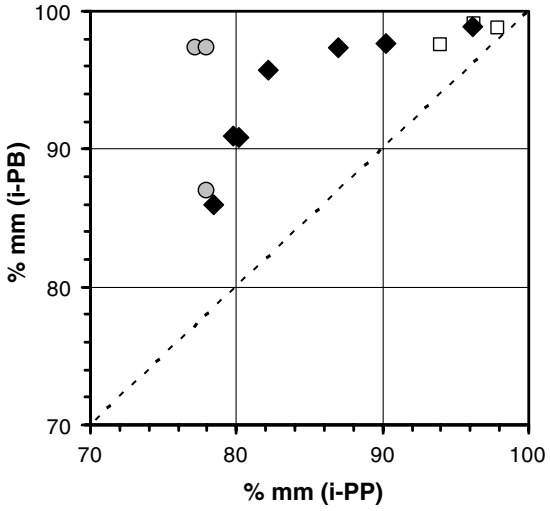

Fig. 1. Comparison of isotactic triad content (% *mm*) of polybutenes and polypropenes from C_2-symmetric (□), bis(2-methylthieno)Cp-based C_1-symmetric (♦) and fluorenyl-based C_1-symmetric (◉) zirconocenes.

Table 1
Stereoselectivity of C_2-symmetric and C_1-symmetric zirconocenes: propene vs. 1-butene[a]

	Metallocene	iPP		iPB	
		% *mm*	% *mmmm*	% *mm*	% *mmmm*
1	*rac*-Me_2Si(2-MeInd)$_2ZrCl_2$	94.0	90.2	97.6	96.0
	rac-Me_2Si(2-MeBenz[e]Ind)$_2ZrCl_2$	96.3	93.8	99.1	98.5
	rac-H_2C(3-^{t}BuInd)$_2ZrCl_2$	97.9[b]	96.5[b]	98.8[b]	98.1[b]
2	Me_2Si(2-MeInd)(9-Flu)$ZrCl_2$	78.0[c]	68.2[c]	87.0[c]	79.5[c]
3	Me_2Si(2,4,6-Me_3Ind)(9-Flu)$ZrCl_2$	77.2[c]	64.8[c]	97.4[c]	95.8[c]
3a	Me_2Si(2,4,6-Me_3Ind)(9-Flu)$ZrMe_2$	78.0[c]	66.0[c]	97.4[c]	95.7[c]
	Me_2Si(Ind)(BMTCp)$ZrCl_2$	78.4[b]	66.6[b]	86.0	77.7
4	Me_2Si(2-MeInd)(BMTCp)$ZrCl_2$	79.8	68.6	90.9	85.4
	Me_2Si(2-MeBenz[e]Ind)(BMTCp)$ZrCl_2$	82.2	72.1	95.7	92.9
	Me_2Si(4,7-Me_2Ind)(BMTCp)$ZrCl_2$	80.2	69.2	90.8	85.1
	Me_2Si(2,4,7-Me_3Ind)(BMTCp)$ZrCl_2$	90.2	84.2	97.7	96.2
5	Me_2Si(2,4,6-Me_3Ind)(BMTCp)$ZrCl_2$	87.0	79.3	97.4	95.7
	Me_2Si[2-Me-4-(α-naphthyl)Ind](BMTCp)$ZrCl_2$	96.2	93.7	98.8	98.0

[a] Polymerization tests in liquid monomer, T_p = 70 °C, 60 min, Al_{MAO}/Zr = 500, with Al^{i}Bu$_3$ as scavenger (2 and 6 mmol for propene and 1-butene, respectively). ^{13}C NMR at 100 MHz. When regioirregularities are present, % *mmmm* and % *mm* values are calculated on primary units only. BMTCp = bis(2-methylthieno)cyclopentadienyl.
[b] T_p = 60 °C.
[c] ^{13}C NMR at 150 MHz.

2.2. QM/MM study of the stereoselectivity in propene and 1-butene polymerization

As shown above, a remarkable feature of the zirconocene catalysts is the increase in enantioface selectivity in 1-butene vs. propene polymerization. We decided to investigate the origin of this effect by means of a molecular modeling study of the selectivity of the insertion of propene and 1-butene on the Zr-polymeryl species generated from the C_2- and C_1-symmetric catalysts **1**–**5** shown in Chart 1.

Geometries of the transition structures for the insertion of the olefin into the Zr–C σ-bond were computed by means of an integrated QM/MM model (see Section 4). The alkyl groups used to model the polypropene and polybutene growing chains were 2-methylpropyl and 2-ethylbutyl, respectively. Enantioselectivity ($\Delta\Delta E^{\ddagger}$) was computed as the energy difference between the transition structures for the insertion of the "correct" and the "wrong" olefin enantiofaces [1]. For this purpose single-point B3LYP/DZP energy values were used. The computed selectivities were also converted into isotactic triad intensities (% *mm*), to be compared with the corresponding experimental values obtained from the ^{13}C NMR spectra of the polymers [11].

In the following, without losing generality, we consider the (*R,R*) enantiomer of the C_2-symmetric species **1** and the (*R*) enantiomers of the asymmetric species **2**–**5** (these enantiomers are the ones depicted in Chart 1). As a consequence of this choice, the correct and the wrong olefin enantiofaces are the *re* and *si* ones, respectively.

2.2.1. Enantioselectivity for the C_2-symmetric zirconocene *1*

We first analyze the behavior of the C_2-symmetric bisindenyl *ansa*-zirconocene **1**, in which the two coordination sites are identical. Fig. 2 reports the optimized transition structures for the propene insertion into the polypropene growing chain with both the correct (*re*) and the wrong (*si*) enantioface (in the latter case two structures are shown).

The structure in which propene is coordinated with the *re* face (**1a**) is the most stable. The higher stability of this structure can be attributed to the orientation of the growing chain, that develops freely in an open sector, and to the *trans* disposition of the chain and the methyl substituent of the olefin with respect to the reaction plane. Both this structural features lead to a reduced repulsive interaction between the *ansa*-ligand, the growing chain, and the olefin.

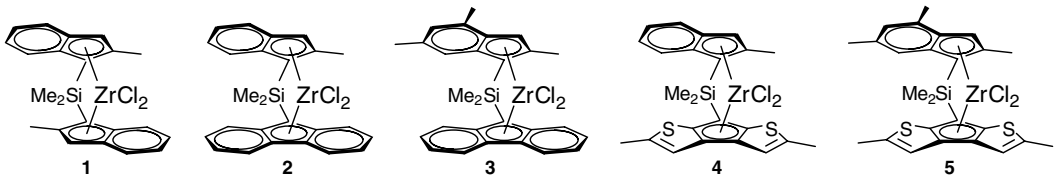

Chart 1.

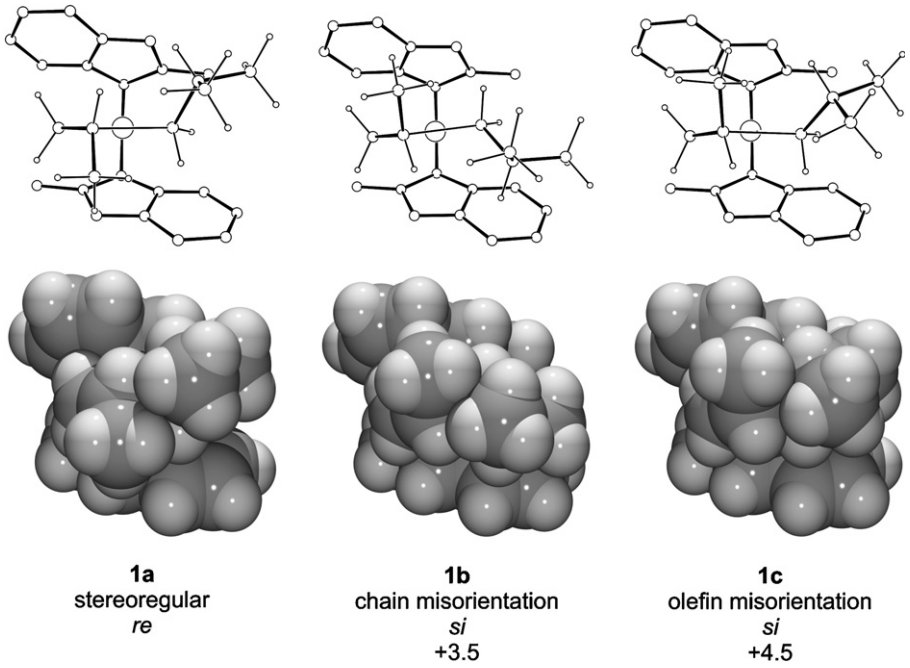

Fig. 2. Transition structures and relative energies (kcal mol^{-1}) for the stereoregular and irregular insertion of propene for catalyst **1**. The silicon-bound methyl groups have been omitted for clarity.

Olefin misinsertion can be due to chain misorientation or to olefin misorientation [12]. In the first case the growing chain develops in a crowded sector (instead of an open one), while in the second case the olefin substituent and the growing chain are placed in a *cis* disposition (instead of a *trans* one) with respect to the reaction plane. We computed the transition structures for the two possible mechanisms of olefin misinsertion (**1b** and **1c**, respectively). Chain misorientation resulted to be more favored over olefin misorientation by 1.0 kcal mol^{-1}. It is interesting to note that if we consider the stage of olefin coordination (i.e. the corresponding alkyl olefin complexes) the reverse is true (by 3.3 kcal mol^{-1}) since, due to the higher distance between the olefin and the growing chain, steric repulsion arises almost exclusively from the *ansa*-ligand-growing chain interactions and not from the interaction between the olefin and the growing chain. However, in order to determine enantioselectivity the lower energy transition structure must be taken into account and in the following only the chain misorientation mechanism will be considered. The structure corresponding to propene insertion with the *si* face is thus destabilized by the unfavorable steric interactions between the *ansa*-ligand and the wrongly oriented growing chain of the polymer.

A similar situation was found for the insertion of 1-butene into the polybutene growing chain. However, the computed enantioselectivity for propene (3.5 kcal mol^{-1}) is somewhat lower than that for 1-butene (4.2 kcal mol^{-1}). The isotactic triad contents (% *mm*) computed from these values for polypropene and polybutene (98.2% and 99.4%, respectively) are in fair agreement with the experimental observations (94.0% and 97.6%) [13].

To better identify the factors determining the origin of the enhanced enantioselectivity of the insertion of 1-butene with respect to propene we studied two mixed processes, i.e. the insertion of propene into the growing chain of polybutene and the insertion of 1-butene into the growing chain of polypropene. The computed enantioselectivities for the two processes are 4.0 and 3.7 kcal mol^{-1}, respectively.

It is interesting to note that the insertion of a given olefin into the growing chain of polybutene is always more stereoselective (by 0.5 kcal mol^{-1}) than the insertion of the same olefin into the growing chain of polypropene. Moreover, the insertion of butene into a given growing chain is always more selective (by 0.2 kcal mol^{-1}) than the insertion of propene into the same growing chain. From this findings we can conclude that both the size of (the last inserted unit of) the growing chain *and* the size of the olefin substituent contribute to determine the enhanced enantioselectivity of the 1-butene insertion process, the former playing a major role.

This result is in accordance with the broadly accepted fact that the source of enantioselectivity in the polymerization of propene, with both chiral stereorigid metallocenes and heterogeneous Ti-based Ziegler-Natta catalysts, is the chiral orientation of the growing chain [14]. However, due to the larger size of 1-butene, the effect of a direct interaction between the *ansa*-ligand and the olefin becomes appreciable as well [15].

2.2.2. Enantioselectivity for the C_1-symmetric zirconocenes 2–5

The most important feature of C_1-symmetric zirconocenes is that their two coordination sites are nonequivalent. As a consequence, the enantioselectivity of two consecutive olefin insertion steps are (in general) different, since the selectivity of the two sites are non constrained by symmetry to be equal (like in C_2-symmetric catalysts) or opposite (like in the syndioselective C_s-symmetric catalysts). Moreover, the structures corresponding to the binding of the olefin at the two nonequivalent coordination sites (in the following labeled *inward* and *outward*, according to the position of the monomer with respect to the pocket defined by the *ansa*-ligand) can have a significantly different stability. In this case the sequence of chain migratory steps can be altered, because after an insertion step at the *inward* site, in the absence of a coordinated monomer molecule, the growing chain can swing back to the previous, more stable, position (back-skip of the growing chain) [16].

As a consequence, these catalysts can vary in stereoselectivity from hemiisospecific to isospecific, depending on the substituents on the *ansa*-ligand that define the enantioselectivity of the two alternating sites *and* the probability of back-skip. Enantioselectivities at the two coordination sites can be easily computed. At variance, a quantitative comparison of back-skip and insertion activation energies is very difficult due to the different nature of the process at study. In particular, the two processes have different molecularities and an accurate estimation of the entropic cost of binding the olefin (in solution and in presence of a counterion) is mandatory [16b].

The computed enantioselectivities for the insertion of propene and 1-butene at both the inward- and outward-olefin sites of zirconocenes **2**–**5** are reported in Table 2, along with the data for the C_2-symmetric species **1** (for which the two sites are identical). Fig. 3 reports the optimized transition structures for the stereoregular and irregular insertion of propene at both the inward- and outward-olefin site for catalyst **2**.

Enantioselectivities computed for the inward-olefin site of the fluorenyl derivatives **2** and **3** are high and comparable to that of the C_2-symmetric zirconocene **1**. This result is expected, since the steric interactions at work are similar. However, it is interesting to note that the enantioselectivity slightly decreases on passing from **1** to **2** and, at variance, increases on passing to **3**. This behavior is consistent with the presence of a secondary effect attributable to the direct interaction of the olefin with the *ansa*-ligand, since the factors determining the orientation of the growing chain in the more open sector of the catalyst are approximately the same in all the three species.

For the outward-olefin site the computed enantioselectivities are much lower, as a consequence of a reduced

Table 2
Computed enantioselectivities ($\Delta\Delta E^{\ddagger}$) and computed and experimental isotactic triad contents (% *mm*) for propene and 1-butene polymerization with zirconocenes **1**–**5**

Metallocene	Olefin	$\Delta\Delta E^{\ddagger}_{inw}$ (kcal mol^{-1})	$\Delta\Delta E^{\ddagger}_{out}$ (kcal mol^{-1})	% *mm* back-skip	% *mm* no back-skip	% *mm* exp.[a]
1	Propene	3.5[b]			$98._2$ [c]	94.0
	1-Butene	4.2[b]			$99._4$ [c]	97.6
2	Propene	3.2	0.5	$97._1$	$57._1$	78.0
	1-Butene	3.9	0.7	$99._0$	$64._4$	87.0
3	Propene	4.1	1.2	$99._3$	$79._7$	77.2
	1-Butene	4.6	1.8	$99._6$	$89._8$	97.4
4	propene	3.5	0.3	$98._2$	$45._7$	79.8
	1-Butene	4.1	0.5	$99._3$	$56._6$	90.9
5	Propene	4.3	0.8	$99._5$	$66._5$	87.0
	1-Butene	4.8	1.2	$99._7$	$77._9$	97.4

[a] Experimental values from Table 1.
[b] The two coordination sites of **1** are identical.
[c] The occurence of back-skip is irrelevant in determining the isotactic triad contents for **1**.

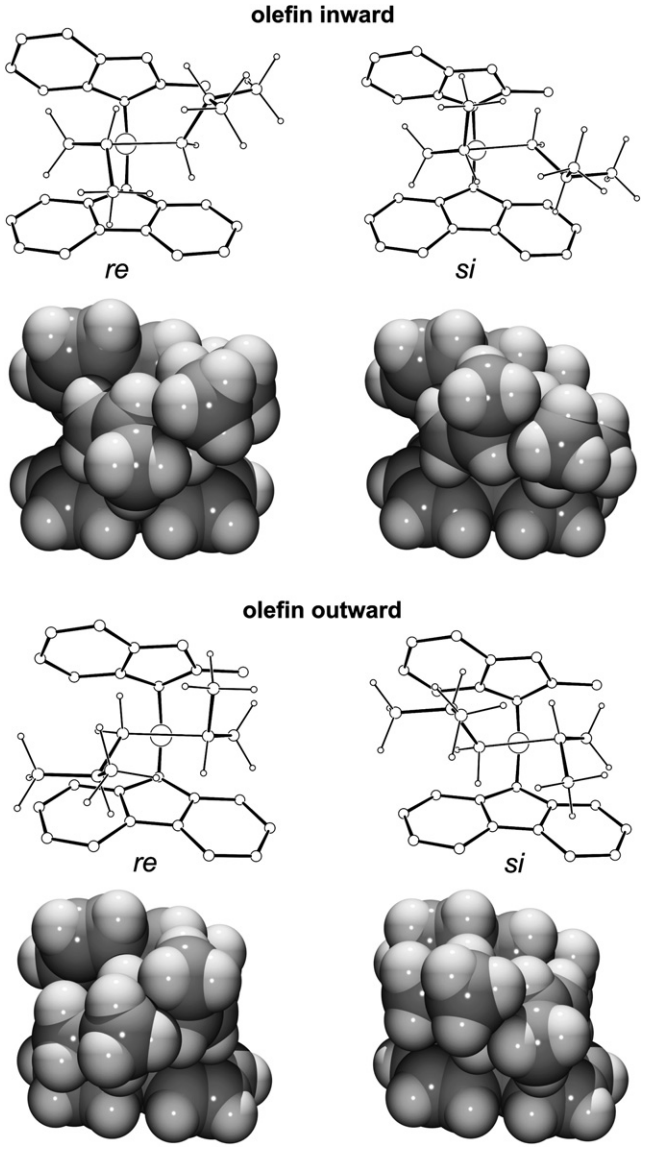

Fig. 3. Transition structures for the stereoregular and irregular insertion of propene for catalyst **2** at both the inward- and outward-olefin site. The silicon-bound methyl groups have been omitted for clarity.

energy difference between the two orientations of the growing chain inside the pocket of the *ansa*-ligand.

The dithienocyclopentadienyl derivatives **4** and **5** are more enantioselective than their fluorenyl counterparts at the inward-olefin site, but at the outward-olefin site the contrary holds. These two findings seem to conflict with each other. They can be understood if we admit that the heterocyclic ligand is sterically more demanding than the fluorenyl ligand. This assumption leads to an enhanced selectivity at the site in which the heterocyclic group directly induces the growing chain orientation (the inward-olefin) but to a lowered selectivity at the site in which it indirectly acts as an opposing group to the indenyl ligand. This result does not conform to the finding of Ewen that *unsubstituted* thienocyclopentadienyl derivatives are less enantioselective than their indenyl analogues [17]. However, the methyl group adjacent to the sulfur atom in **4** and **5** can be responsible of the opposite behavior here observed. Indeed, a zirconocene similar to **4** but lacking the α-methyl groups shows a significantly reduced selectivity in propene polymerization (70.4% *mm*) [7].

As expected, selectivity significantly grows on passing from the 2-methylindenyl derivatives (**2** and **4**) to the 2,4,6-trimethylindenyl derivatives (**3** and **5**).

The insertion of 1-butene is always more selective than that of propene for all the zirconocenes. The difference between insertion selectivity for the two olefins ranges from 0.2 (for the outward site of **2** and **4**) to 0.7 kcal mol^{-1} (for the inward site of **2**).

Since, as previously stated, a computational comparison of back-skip and insertion activation energies is difficult and quantitatively not much reliable, in order to derive the isotactic triad contents from the computed enantioselectivities some assumptions about back-skip have to be made. Values computed in the two limiting situations (i.e. assuming that back-skip occurs after each insertion or that it never occurs) are reported in Table 2. By comparing these computed limiting values with the experimental triad distributions some conclusions can be drawn. In particular, back-skip seems to be always present in 1-butene polymerization (we can

estimate a back-skip probability of about 0.8–0.9 for catalysts **2**–**5**). In the case of propene, back-skip is not likely to occur for the fluorenyl derivative **3** whereas we can estimate a back-skip probability of about 0.8 for the dithieno Cp complexes **4** and **5** [18]. These findings are in accordance with the known positive correlation between back-skip occurrence and steric hindrance, once again if we admit that the heterocyclic ligand is sterically more demanding than the fluorenyl ligand.

For bent-metallocene catalysts, the 'bite angle' [19] is usually taken as an indirect measure of the steric pressure exerted by the *ansa*-ligand. Values computed for the dithienocyclopentadienyl derivatives **4** and **5** (63.2° and 63.4°, respectively) are only slightly greater than those computed for the fluorenyl derivatives **2** and **3** (61.9° and 62.0°, respectively). As it has been previously observed [20], the bite angle is very sensitive to differences in the number and type of the *ansa*-atoms, while it is almost unaffected by changes in the nature and the substitution pattern of the π-ligands, which lead only to minor modifications in the local geometry around the metal atom. As a consequence, it is not easy to forecast the polymerization behavior of a catalyst only on the basis of structural parameters of the zirconocene.

3. Conclusions

According to the large set of data now available, 1-butene polymerization with C_1-symmetric zirconocene catalysts is confirmed to be significantly more stereoselective than propene polymerization. A less pronounced stereoselectivity enhancement can be confirmed for C_2-symmetric zirconocene catalysts as well.

QM/MM calculations allow to attribute this behavior mainly to the larger size of the growing chain of polybutene with respect to polypropene, in agreement with the well known site control mechanism operating through the chiral orientation of the growing chain [21]. However, by comparing the energy barriers of some 'mixed' insertion processes, a secondary effect due to a *direct* steric interaction between the olefin and the *ansa*-ligand has been identified.

By comparing the computed selectivities with the observed triad distributions for the C_1-symmetric catalysts, the importance of back-skip has been revealed. Indeed, the larger enantioselectivity computed for 1-butene at both the inward and the outward sites cannot by itself account for the enhanced isotacticities observed for polybutene with respect to polypropene and an apparent greater propensity of the polybutene growing chain to back-skip must be accepted.

4. Experimental

4.1. Computational details

Geometries were optimized at the ONIOM level of theory [22]. In this integrated method the molecular system being studied is divided into two layers which are treated with different model chemistries. The results are then automatically combined into the final predicted results. In the present work the model system was the $[H_2SiCp_2Zr(ethyl)(propene)]^+$ cation, which was treated at the HF level. A basis set incorporating the "small core" effective core potentials of Hay and Wadt was used for silicon and zirconium along with valence double-ζ functions (LanL2DZ). The standard valence double-ζ basis set 3-21G was used for carbon and hydrogen [23]. The remaining parts of the molecules were treated by molecular mechanics, employing the Universal Force Field without the electrostatic term [24]. Default scale factors were employed to determine bond distances between atoms in the real system and their link atoms in the model system [22f]. The partition of the systems under study between the QM and MM parts is shown in Fig. 4, using the $[Me_2Si(2\text{-}MeInd)_2Zr(2\text{-}ethylbutyl)(1\text{-}butene)]^+$ cation as an example. The structures of the dimethyl derivatives of all the catalysts were previously optimized at the same level. For these calculations the model system was $[H_2SiCp_2ZrMe_2]$.

Transition structures were located using the STQN method. Geometries were optimized in redundant internal coordinates until the maximum (root-mean-square) force was less than 0.00045 (0.00030) a.u. Calculations were done without the imposition of any symmetry. Analytic frequency computations were done to check the nature (true minima or transition-state) of all the stationary points.

Single-point energy were subsequently computed at the B3LYP level. A basis set incorporating the "small core" effective core potentials of Hay and Wadt was used for silicon, sulfur, and zirconium along with valence double-ζ functions (LanL2DZ) augmented with a single polarization function ($\alpha_{d,Si} = 0.45$, $\alpha_{d,S} = 0.65$, $\alpha_{f,Zr} = 0.875$ [25]). The standard valence double-ζ basis set with a single polarization function 6-31G(d,p) was used for all remaining atoms. All the computations were performed with GAUSSIAN 03 [26].

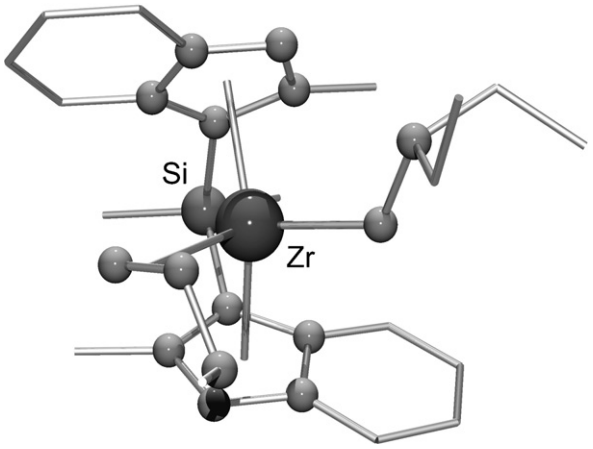

Fig. 4. Schematic view of the $[Me_2Si(2\text{-}MeInd)_2Zr(2\text{-}ethylbutyl)(1\text{-}butene)]^+$ cation, in which the QM (ball and stick) and the MM (stick) parts are highlighted. Hydrogen atoms have been omitted for clarity.

Table 3
Propene and 1-butene polymerization tests with **3**/MAO and **3a**/MAO[a]

Metallocene	Olefin	MC (mg)	Activity (kg/g_{MC}/h)	$\overline{M}_v$[b]	T_m (°C)	% *mm* [c]	% *mmmm*[c]
3	Propene	1	38	149000	109.5	77.1_5	64.8
3a	Propene	1	39	134000	107.8	77.9_9	66.0
3	1-Butene	3.0	14	309000	98.4	97.4_4	95.8
3a	1-Butene	4.1	12	284000	97.1	97.4_1	95.7

[a] Polymerization tests in liquid monomer, $T_p = 70$ °C, 60 min, $Al_{MAO}/Zr = 500$, with Al^iBu_3 as scavenger (2 and 6 mmol for propene and 1-butene, respectively). MC = metallocene.
[b] Viscosity average molecular weights were obtained from intrinsic viscosity measurements (tetrahydronaphthalene, 135 °C).
[c] NMR data were obtained at 150 MHz.

Conversion of the computed enantioselectivities into triad intensities was done assuming enantiomorphic site control and a polymerization temperature of 70 °C. A Monte Carlo simulation of 100 polymer chains each containing 1 000 000 stereocenters was employed. This conversion can also be done on the basis of Markov chain matrix mathematics [27].

4.2. Polymer syntheses and characterization

Detailed metallocene syntheses, and polymerization and polymer analysis procedures can be found in Refs. [7] (polypropene) and [8] (polybutene). Me_2Si(2-MeInd)(9-Flu)$ZrCl_2$ (**2**) has been prepared following the protocol in Ref. [9], Me_2Si(2,4,6-Me_3Ind)(9-Flu)$ZrMe_2$ (**3a**) has been prepared as described in Ref. [10].

^{13}C NMR spectra were acquired on a *Bruker Av-600* spectrometer operating at 150.91 MHz in the Fourier transform mode at 120 °C. The samples were dissolved in 1,1,2,2-tetrachloroethane-d_2 at 120 °C with a 8% wt/vol concentration. Each spectrum was acquired with a 90° pulse, 15 s of delay between pulses and CPD (WALTZ 16) to remove ^1H–^{13}C coupling. 1500 transients were stored in 32 K data points using a spectral window of 9000 Hz.

The peaks of the *mmmm* CH_3 carbon for iPP and of the *mmmm* CH_2 carbon of the ethyl branch for iPB were used as internal reference at 21.8 ppm and 27.73 ppm, respectively. The polymerization results for **3**/MAO and **3a**/MAO are listed in Table 3.

Acknowledgements

We thank Ms. Cristina Fiori for the synthesis of **2**, Dr. Iolanda Santoriello for the synthesis of **3a**, the Polymerization Laboratory and the Analytical Department of the Giulio Natta Research Centre of Basell Polyolefins in Ferrara for polymer synthesis and characterization.

References

[1] L. Resconi, L. Cavallo, A. Fait, F. Piemontesi, Chem. Rev. 100 (2000) 1253, and references therein.
[2] N. Herfert, G. Fink, Macromol. Symp. 66 (1993) 157.
[3] N. Naga, K. Mizunuma, Macromol. Rapid Commun. 18 (1997) 581.
[4] A. Borriello, V. Busico, R. Cipullo, O. Fusco, J.C. Chadwick, Macromol. Chem. Phys. 198 (1997) 1257.
[5] L. Resconi, L. Abis, G. Franciscono, Macromolecules 25 (1992) 6814.
[6] F. Grisi, P. Longo, A. Zambelli, J.A. Ewen, J. Mol. Catal. A: Chem. 140 (1999) 225.
[7] L. Resconi, S. Guidotti, I. Camurati, R. Frabetti, F. Focante, I.E. Nifant'ev, I.P. Laishevtsev, Macromol. Chem. Phys. 206 (2005) 1405.
[8] L. Resconi, I. Camurati, F. Malizia, Macromol. Chem. Phys. 207 (2006) 2257.
[9] J. Kukral, P. Lehmus, T. Feifel, C. Troll, B. Rieger, Organometallics 19 (2000) 3767.
[10] L. Resconi, S. Guidotti, I. Santoriello, Int. Pat. Appl. WO 2006/117285 to Basell.
[11] K. Angermund, G. Fink, V.R. Jensen, R. Kleinschmidt, Chem. Rev. 100 (2000) 1457, and reference therein.
[12] (a) M. Borrelli, V. Busico, R. Cipullo, S. Ronca, P.H.M. Budzelaar, Macromolecules 35 (2002) 2835;
(b) M. Borrelli, V. Busico, R. Cipullo, S. Ronca, P.H.M. Budzelaar, Macromolecules 36 (2003) 8171.
[13] It is important to realize that uncertainties in computed relative energy barriers can be as high as 1 kcal mol^{-1} (leading to a difference in computed isotacticities of 5%). In addition, errors as high as 1% are typical for triad distributions measured by ^{13}C NMR.
[14] (a) P. Corradini, G. Guerra, L. Cavallo, Top. Stereochem. 24 (2003) 1;
(b) A.K. Rappé, W.M. Skiff, C.J. Casewit, Chem. Rev. 100 (2000) 1435.
[15] (a) P. Longo, A. Grassi, C. Pellecchia, A. Zambelli, Macromolecules 20 (1987) 1015;
(b) P. Longo, A. Proto, A. Grassi, P. Ammendola, Macromolecules 24 (1991) 4624.
[16] (a) S.A. Miller, J.E. Bercaw, Organometallics 25 (2006) 3576;
(b) M. Graf, K. Angermund, G. Fink, W. Thiel, V.R. Jensen, J. Organomet. Chem. 691 (2006) 4367;
(c) G. Guerra, L. Cavallo, G. Moscardi, M. Vacatello, P. Corradini, Macromolecules 29 (1996) 4834.
[17] J.A. Ewen, R.L. Jones, M.J. Elder, A.L. Rheingold, L.M. Liable-Sands, J. Am. Chem. Soc. 120 (1998) 10786.
[18] A very similar behavior has been previously reported for propene polymerization with [Me_2C(3-^{t}BuCp)(9-Flu)$ZrCl_2$] and [Me_2C(3-^{t}-BuCp)(BTCp)$ZrCl_2$] (BTCp = dithienocyclopentadienyl) J.A. Ewen, R.L. Jones, M.J. Elder, in: W. Kaminsky (Ed.), Metalorganic Catalysts for Synthesis and Polymerisation, Springer-Verlag, Berlin, 1999, p. 150.
[19] The bite angle is the angle between the planes defined by the two five-membered rings bound to the metal atom. The reported values were computed for the dimethyl derivatives of compounds **2**–**5**.
[20] V.A. Dang, L.-C. Yu, D. Balboni, T. Dall'Occo, L. Resconi, P. Mercandelli, M. Moret, A. Sironi, Organometallics 18 (1999) 3781.
[21] P. Corradini, G. Guerra, Prog. Polym. Sci. 16 (1991) 239, and references therein.
[22] (a) F. Maseras, K. Morokuma, J. Comput. Chem. 16 (1995) 1170;
(b) S. Humbel, S. Sieber, K. Morokuma, J. Chem. Phys. 105 (1996) 1959;

(c) T. Matsubara, S. Sieber, K. Morokuma, Int. J. Quant. Chem. 60 (1996) 1101;
(d) M. Svensson, S. Humbel, R.D.J. Froese, T. Matsubara, S. Sieber, K. Morokuma, J. Phys. Chem. 100 (1996) 19357;
(e) M. Svensson, S. Humbel, K. Morokuma, J. Chem. Phys. 105 (1996) 3654;
(f) S. Dapprich, I. Komáromi, K.S. Byun, K. Morokuma, M.J. Frisch, J. Mol. Struct. (Theochem) 462 (1999) 1;
(g) T. Vreven, K. Morokuma, J. Comput. Chem. 21 (2000) 1419.

[23] Following the suggestion of a reviewer, we checked the reliability of our approach by re-optimizing the transition-state geometries for one particular catalyst (**1**) using B3LYP as the core method for the ONIOM approach. We found geometries similar to those computed using HF (bond lengths change by 0.01 Å at most). More importantly, the computed $\Delta\Delta E^{\ddagger}$ values change by 0.2 kcal mol^{-1} at most.

[24] (a) A.K. Rappé, C.J. Casewit, K.S. Colwell, W.A. Goddard III, W.M. Skiff, J. Am. Chem. Soc. 114 (1992) 10024;
(b) K. Gundertofte, T. Liljefors, P.-O. Norrby, I. Pettersson, J. Comp. Chem. 17 (1996) 429.

[25] W. Ehlers, M. Böhme, S. Dapprich, A. Gobbi, A. Höllwarth, V. Jonas, K.F. Köhler, R. Stegmann, A. Veldkamp, G. Frenking, Chem. Phys. Lett. 208 (1993) 111.

[26] GAUSSIAN 03 (Revision C.02), Gaussian Inc., Wallingford, CT, 2004.

[27] V. Busico, R. Cipullo, P. Corradini, L. Landriani, M. Vacatello, A.L. Segre, Macromolecules 28 (1995) 1887.